



## Sensitivity of time-dependent density functional theory to initial conditions

Aurel Bulgac <sup>1</sup>, Ibrahim Abdurrahman,<sup>1</sup> and Gabriel Włazłowski <sup>2,1</sup>

<sup>1</sup>*Department of Physics, University of Washington, Seattle, Washington 98195–1560, USA*

<sup>2</sup>*Faculty of Physics, Warsaw University of Technology, Ulica Koszykowa 75, 00–662 Warsaw, Poland*



(Received 28 August 2021; accepted 16 March 2022; published 4 April 2022)

Time-dependent density-functional theory is mathematically formulated through nonlinear coupled time-dependent three-dimensional partial differential equations, and it is natural to expect a strong sensitivity of its solutions to variations of the initial conditions, akin to the butterfly effect ubiquitous in classical dynamics. Since the Schrödinger equation for an interacting many-body system is, however, linear and mathematically the exact equations of the density-functional theory reproduce the corresponding one-body properties, it would follow that the Lyapunov exponents are also vanishing within a density-functional theory framework. Whether for realistic implementations of the time-dependent density-functional theory the question of the absence of the butterfly effect and whether the dynamics provided is indeed a predictable theory was never discussed. At the same time, since the time-dependent density-functional theory is a unique tool allowing us to study the nonequilibrium dynamics of strongly interacting many-fermion systems, the question of predictability of this theoretical framework is of paramount importance. Our analysis, for a number of quantum superfluid many-body systems (unitary Fermi gas, nuclear fission, and heavy-ion collisions) with a classical equivalent number of degrees of freedom  $O(10^{10})$  and larger, suggests that its maximum Lyapunov exponents are negligible for all practical purposes.

DOI: [10.1103/PhysRevC.105.044601](https://doi.org/10.1103/PhysRevC.105.044601)

### I. PREAMBLE

Dynamical systems are often deterministic but at the same time unpredictable in the long run. In 1884 Gösta Mittag-Leffler initiated the idea of a new international prize in mathematics in honor of King Oscar II of Sweden and Norway. The first challenge was to solve the  $N$ -body problem interacting according to Newton's law of gravitation. In 1888 Henri Poincaré submitted his answer, about 300 hand-written pages, to which upon request he added another 100 or so hand-written pages, and he was awarded the prize. The initial Poincaré “solution” had an error, he missed what we now know as the butterfly effect, an error which he fixed before his results were later published [1]. The entire dramatic story is available online [2]. Poincaré's insights were further extended by the work of Lyapunov [3], who introduced the now ubiquitous Lyapunov exponents. The topic remained practically dormant until the paper of Lorenz [4], who soon after apparently introduced the meme butterfly effect as a poetic illustration of the high sensitivity of deterministic systems to initial conditions. This is how we have learned that the equations of motion of a physical system can be deterministic and at the same time can be unpredictable in the long run. The chaos theory was born before anyone had any clue that quantum mechanics would quite soon change the world in so many ways, and in particular our interpretation of chaos. Recently, a statistical approach was suggested as an alternative reformulation of the three-body problem challenge [5–8], which renders this problem deterministic.

Classical chaos studies show that a system of interacting particles, being nonlinear in character, would typically show sensitivity to initial conditions. Unless a classical Hamiltonian system is integrable it is characterized by the presence of at least one positive Lyapunov exponent, rendering any long-time predictions totally unreliable, even though the equations of motion are unquestionably deterministic. Popularly this is referred to as the butterfly effect and in scientific literature as deterministic chaos. If the time-dependent density-functional theory (TDDFT), which by default is a nonlinear theory, unlike the many-body Schrödinger equation, would be sensitive to initial conditions, the TDDFT would be unpredictable and useless as a theoretical tool. The sensitivity of a many-body system to initial conditions would be equivalent to the absence of the linear regime, as any small initial perturbation would increase exponentially in time and the many-body system would be basically unstable.

Our goal is to ascertain whether the TDDFT equations are characterized by nonvanishing Lyapunov exponents.

### II. QUANTUM MECHANICS VERSUS CLASSICAL MECHANICS

In this section we review a number of aspects of chaos theory in the classical and quantum descriptions of nature, which can be skipped by the informed reader.

The Lyapunov exponent  $\lambda$  of a dynamical system is a quantity which characterizes the rate of separation of initially

infinitesimally close trajectories:

$$\lambda = \lim_{t \rightarrow \infty} \lambda(t) = \lim_{t \rightarrow \infty} \frac{1}{t} \ln \frac{|\delta \mathbf{Z}(t)|}{|\delta \mathbf{Z}(0)|}, \quad (1)$$

where  $\delta \mathbf{Z}(t)$  are the differences between the two full sets of phase-space variables. In practice one evaluates  $\lambda$  via Eq. (1) by starting from a fixed small  $|\delta \mathbf{Z}(0)|$  and by evolving in time the system for a relatively long time. For an  $N$ -dimensional  $\mathbf{Z}(t)$  one defines a spectrum of  $N$  Lyapunov exponents. In the case of a Hamiltonian dynamics, Liouville's theorem implies that

$$\sum_{k=1}^N \lambda_k = 0, \quad (2)$$

and, moreover, that a number of these Lyapunov exponents identically vanish in the presence of symmetries and conserved quantities. In the case of dissipative dynamics  $\sum_{k=1}^N \lambda_k < 0$ . The sum of all positive Lyapunov exponents gives an estimate of the Kolmogorov-Sinai entropy [9]. A related quantity is the Lyapunov dimension or Kaplan-Yorke dimension [10].

A particular class of classical systems is interesting in connection with quantum dynamics: for any quadratic Hamiltonian in the canonical coordinates and momenta all the Lyapunov exponents are identically zero. It is trivial to show that the nonrelativistic quantum dynamics with instantaneous interactions between particles is mathematically equivalent to a classical system of infinitely many coupled harmonic oscillators. If a quantum  $N$ -body system with coordinates  $x = (\mathbf{r}_1, \dots, \mathbf{r}_N)$  satisfies the time-dependent Schrödinger equation

$$i\hbar \dot{\Psi}(x, t) = \int dy H(x, y) \Psi(y, t), \quad (3)$$

then one can introduce the continuous classical canonical coordinates and momenta, similarly to fluid dynamics [11], and the corresponding total Hamiltonian of the ‘‘classical’’ continuum canonical coordinates. We suppressed, for the sake of simplicity, the spin, isospin, and any other discrete degree of freedom (DoF). A set of continuous canonical coordinates and momenta convenient for our purpose is

$$q_x(t) = \sqrt{2} \operatorname{Re} \Psi(x, t), \quad (4)$$

$$p_x(t) = \sqrt{2} \operatorname{Im} \Psi(x, t), \quad (5)$$

$$\mathcal{H} = \frac{1}{\hbar} \int dx dy \Psi^*(x, t) H(x, y) \Psi(y, t), \quad (6)$$

where  $\mathcal{H}$  is the corresponding classical Hamiltonian of quadratic form, and where  $x$  labels these canonical coordinates. Using the classical Poisson brackets one immediately obtains the classical Hamiltonian form of the Schrödinger equation:

$$\dot{q}_x(t) = \{q_x(t), \mathcal{H}\} = \frac{\delta \mathcal{H}}{\delta p_x(t)}, \quad (7)$$

$$\dot{p}_x(t) = \{p_x(t), \mathcal{H}\} = -\frac{\delta \mathcal{H}}{\delta q_x(t)}. \quad (8)$$

This Hamiltonian form of the Schrödinger equation naturally implies that all Lyapunov exponents of any nonrelativistic many-body Hamiltonian with instantaneous interactions identically vanish, and thus it strictly follows that there is no quantum chaos, or there is no sensitivity to the initial conditions for any quantum many-body problem with instantaneous interactions. Alternatively, one can state that the Schrödinger equation is linear and thus no exponential divergence between initially close quantum states can be observed.

This is the reason why, for many decades now, theorists tried to answer such questions using argumentation based on the correspondence principle: Why a quantum Hamiltonian, which in the classical limit  $\hbar \rightarrow 0$  has chaotic dynamics, does not show any sensitivity to initial conditions? How can one identify the signatures of chaotic features present in the classical limit in the quantum description? Most of the studies of quantum chaos focused on several aspects: (i) the presence of either the Poisson or of the random matrix energy-level distributions in quantum systems [12] compared with their corresponding integrable or chaotic classical counterparts [13]; and (ii) the ‘‘scars’’ on the quantum wave functions in the limit  $\hbar \rightarrow 0$  left by the classical periodic orbits [14–18]. Unfortunately, the wave function ‘‘scars’’ cannot be studied in case of quantum many-body systems, for obvious reasons. The role of the boundary effects versus the role of the interaction between particles were not always clearly separated in such studies. In an overwhelming fraction of studies of quantum chaos the object was devoted to billiards, typically in two dimensions. In the present study we concentrate solely on the role of the interaction between particles.

In spite of all the insight gathered during the past several decades in quantum chaos, one did not really put in evidence a sensitivity to initial conditions in a manner as clear as in classical dynamical systems. Recently, a new approach has been advocated: the study of the so-called out-of-time-ordered correlator (OTOC) [19,20], in particular, the quantity

$$C(t) = -\frac{\operatorname{Tr}\{e^{-\beta \hat{H}} [\hat{x}(t), \hat{p}(0)]^2\}}{\hbar^2 \operatorname{Tr}\{e^{-\beta \hat{H}}\}}, \quad (9)$$

where  $[\hat{x}(t), \hat{p}(0)]$  is the commutator of the Heisenberg coordinate and momentum operators

$$\hat{x}(t) = e^{-i\hat{H}t/\hbar} \hat{x}(0) e^{i\hat{H}t/\hbar}, \quad (10)$$

$$\hat{p}(t) = e^{-i\hat{H}t/\hbar} \hat{p}(0) e^{i\hat{H}t/\hbar}, \quad (11)$$

$$[\hat{x}(t), \hat{p}(t)] = i\hbar, \quad [\hat{x}(t), \hat{p}(0)] = i\hbar \frac{\partial \hat{x}(t)}{\partial \hat{x}(0)}, \quad (12)$$

where  $t$  is time and  $\beta = 1/T$  is the inverse temperature. (It is not a requirement to use the canonical average.) The reason for such a choice is that the Poisson bracket  $\{A, B\}$  of the classical limit of the quantum operators  $\hat{A}, \hat{B}$  is related to the quantum commutator

$$\lim_{\hbar \rightarrow 0} \frac{[\hat{A}, \hat{B}]}{i\hbar} = \{A, B\}. \quad (13)$$

One can establish an apparent link between the OTOC and classical chaos and show that the maximum Lyapunov exponent of a quantum system has an upper bound. Maldacena

*et al.* [20], Tsuji *et al.* [21] have proven that, under some very reasonable assumptions,

$$\lambda_{\text{MSS}} = \lim_{t \rightarrow \infty} \frac{\ln C(t)}{2t} \leq \frac{\pi T}{\hbar}. \quad (14)$$

In Ref. [20] the authors overlooked that  $\{x(t), p(0)\} \equiv \partial x(t)/\partial x(0) \propto \exp(\lambda t)$  and thus  $C(t) \propto \exp(2\lambda t)$ . In the classical limit, one discusses the behavior of  $\Delta x_k(t)/\Delta x_k(0) \propto \exp(\lambda t)$ , but not of its square  $|\Delta x_k(t)/\Delta x_k(0)|^2 \propto \exp(2\lambda t)$  because it is done using the OTOC for quantum-mechanical systems, see Eq. (9).

It was shown that the quantum Lyapunov exponent, see Eq. (9), can be extracted from the thermally averaged Loschmidt echo signal [22],

$$L(t) = |\langle \psi | e^{iH_0 t/\hbar} e^{-i(H_0+V)t/\hbar} | \psi \rangle|^2, \quad (15)$$

which exhibits a fast exponential decay  $\propto \exp(-2\lambda t)$ . Here  $V$  stands for a small perturbation—a diagnostic widely used theoretically and experimentally. There is thus a difference between the sensitivity discussed in classical chaos and quantum chaos. In classical systems one perturbs the initial conditions, while in quantum studies one often perturbs the evolution Hamiltonian. Recently, it was argued again, using quantum computing reasoning, that there is no butterfly effect in a genuine quantum evolution [23], as was argued also for decades in the literature.

These various conclusions deserve some introspection.

- (1) Classically, a system manifests a chaotic behavior in isolation, not in contact with a thermal bath, as Maldacena *et al.* [20] have assumed. One can, however, relate the temperature  $T$  used by Maldacena *et al.* [20] with the energy-level density of a (large) quantum system

$$\rho(E) = \text{Tr} \delta(E - H) \propto e^{S(E)}, \quad (16)$$

where  $S(E)$  is the entropy, and then the temperature can be defined as

$$\frac{1}{T} = \frac{dS(E)}{dE} \quad (17)$$

for a large isolated system which reaches statistical equilibrium [24].

The statistical mechanical equilibrium is not an instantaneous quality, so it is difficult to determine from an instantaneous snapshot of the system [24]. The equilibrium characterizes the behavior of a system, in particular of an isolated system, over a very long time, when according to Boltzmann the time average becomes identical to the phase-space average. Thus the time should be long enough for the system to have managed to cover a relevant part of the phase space, for the system to be capable of revealing its statistical equilibrium properties. The equilibration time for a many-body system (assuming extensivity of the system properties) is in theory exponentially large  $\propto e^{\#N}$  as only for a very long time the many-body density matrix of the system reaches equilibrium as a result of visiting all allowed phase-space cells. On the other hand, simple quantities, such as the one-body distribution or the two-body correlations reach equilibrium

in a much shorter time, typically after a relatively small number of interparticle collisions. An interparticle collision can be characterized qualitatively only in a relatively dilute system, and therefore the analysis of dense systems is a qualitatively complicated issue. In dense systems one can replace the particles with quasiparticles and perform a similar analysis. In particular, the entropy increase in time, often discussed in literature, should be evaluated over time intervals longer than the equilibration times.

Equation (9) implicitly assumes that  $C(t)$  is calculated for a system in thermal equilibrium at all times. Since  $C(t)$  increases exponentially, the inverse rate

$$1/\lambda_{\text{MSS}} \gg \tau_{\text{equil}} \quad (18)$$

should be longer than the equilibration rate of the system.

- (2) Classical mechanics appears as a singular limit of quantum mechanics, and very likely the order in which the limits  $\hbar \rightarrow 0$  and  $t \rightarrow \infty$  are taken influence the interpretation of the results of various studies.

In the classical limit there is no upper limit on the maximum value of a Lyapunov exponent, which in a sense explains the abundance of classical chaotic systems, if one is to take the limit  $\hbar \rightarrow 0$  first in Eq. (14). At the same time one can justify why many-body quantum systems do not have random matrix fluctuations on energy scales  $\Delta E$  much larger than the average level separation in large system [25–27],

$$\Delta E \propto T^{3/2} \gg \frac{1}{\rho(E_0)} \approx \exp\left(-\frac{aT}{2}\right), \quad (19)$$

when statistical equilibrium is achieved. This estimate was obtained by considering the behavior of the level density of nonrelativistic many-fermion systems derived by Bethe [28],

$$\rho(E) \propto \exp(\sqrt{aE}), \quad (20)$$

and the corresponding average equilibrium energy and variance

$$E_0 \approx aT^2, \quad \Delta E \propto T^{3/2}, \quad (21)$$

and  $a \approx A/10$ , where  $A$  is the nucleus atomic mass.

- (3) A quantum system can be initialized with any energy  $E$  with an energy width  $\Delta E \ll E$ . Such a packet can likely be chosen to be also rather well localized so as  $\langle \Delta x_k(0) \rangle \langle \Delta p_k(0) \rangle \approx \hbar$ , where  $k = 1, \dots, N$ . It is sufficient to assume that localization is in phase space, and, as in the case of squeezed states,  $\langle \Delta x_k(0) \rangle \propto \hbar^\alpha$  and  $\langle \Delta p_k(0) \rangle \propto \hbar^{1-\alpha}$  or consider any other orientation of such an ellipse or even any other shape with comparable area in the phase space. The more recent hypothesis of eigenstate thermalization and related studies [29–31] are similar approaches to define the relaxation time to reach statistical equilibrium in accordance to the principles of statistical mechanics [24].
- (4) Quantum packets spread with time, and if the system is finite in space, an initial wave packet with a spatial

size smaller than the system size eventually spreads over the entire system during the Ehrenfest time  $\tau_E$ . For a chaotic system, the Ehrenfest time is determined by  $\langle \Delta x_k(0) \rangle \exp(\lambda \tau_E) \approx L$  if one considers the separation of various trajectories in real space. Consider all possible initial conditions of a classical Hamiltonian system in a small volume in phase space of compact size (linear dimensions  $L$  in all directions). If a Hamiltonian system is chaotic and various trajectories diverge exponentially, and since according to Liouville theorem the phase-space volume is conserved, with time this initial compact phase-space volume evolves into a fractal, which can overlap significant parts of the entire phase space.

- (5) One can prepare two identical systems with slightly different initial conditions  $\mathbf{Z}_{1,2}(0)$  and record as a function of time  $\Delta \mathbf{Z}(t) = \mathbf{Z}_1(t) - \mathbf{Z}_2(t)$  and thus extract their relative velocity.

Obviously, the absence of the speed of light in Eq. (14) restricts the validity of this upper bound to nonrelativistic systems only. Since two initially infinitesimally close trajectories cannot separate with a relative speed greater than twice the speed of light, the Lyapunov exponents are strictly vanishing in relativistic theories. Since the linear momenta however can increase indefinitely, the character (and maybe even existence) of chaos in a relativistic system might be qualitatively different from that in a Newtonian system. However, if one would still find a butterfly effect in a relativistic system, when one or a small number of momenta can increase exponentially, a fact that will point likely to the absence of ergodicity. A significant amount of energy will then get concentrated among few degrees of freedom, which will correspond to a relatively small part of phase space.

### III. STRONGLY INTERACTING QUANTUM MANY-BODY SYSTEMS

The main issue we will be concerned with in this work is the presence or absence of chaotic behavior in a quantum many-body system under realistic conditions.

- (1) When analyzing a concrete quantum many-body system and well-specified phenomena, we will assume that the role of  $\hbar \neq 0$  cannot be ignored and therefore we will not consider the  $\hbar \rightarrow 0$  limit.
- (2) For specific physical phenomena, often there is no meaning to consider the limit  $t \rightarrow \infty$ . A typical case is a chemical reaction  $AB + C \rightarrow A + BC$  at later times, after the complex  $BC$  has been formed and it is safely separated from  $A$ . However, by slightly changing the initial conditions, the emerging molecules might end up in drastically different configurations, and this can be interpreted as a significant sensitivity to initial conditions.

It has been established that, for interacting quantum many-body systems, there exist two equivalent quantum-mechanical formulations: the many-body Schrödinger equation and the

density-functional theory (DFT) [32–38], if one is interested only in the behavior of the one-body or the number density of the system  $n(\mathbf{r}, t)$  and the total energy of the system. However, the two formulations, while mathematically proven to be equivalent, have completely different realizations in terms of underlying equations. While the Schrödinger equation is linear and is always equivalent to an infinite continuum system of coupled classical oscillators, DFT is manifestly a nonlinear theory. Since typical implementations of DFT are formulated in terms of single-particle wave functions (spwfs), these spwfs can be in the same manner split into their real and imaginary parts and DFT can be shown to be mathematically equivalent to very complex continuum classical systems governed by nonlinear (nondissipative) classical Hamiltonian equations of motion, similar to Eqs. (7) and (8).

The equivalence of the many-body Schrödinger equation to the TDDFT was proven under a number of assumptions so far [34,36–38], which in practice are not always realized. In particular, Runge and Gross [34] showed that, for a particular choice of initial conditions, one can introduce a density functional, which in an exact DFT formulation also implies the existence of memory terms [37,38]. While even for static DFT formulations, when memory terms are not necessary, the construction of a density functional is still more an art than a science, the density functional for TDDFT should include memory terms and the density functional may depend on the initial conditions as well. Nevertheless, if the collective motion of the many-body system is “adiabatic” one can invoke in practical implementations the adiabatic approximation [37,38] and use a static density functional for a time-dependent problem. This “adiabatic approximation” is used in all, if not the majority of practical implementations of TDDFT and it is the framework adopted in the present study, as also suggested by Runge and Gross [34], see their theorem 4, which leads to a natural extension of the Kohn-Sham scheme [33] to time-dependent problems.

#### A. Upper bounds for the maximum Lyapunov exponents for some quantum many-body nonrelativistic systems

It is instructive to estimate the upper bound for the Lyapunov exponent, Eq. (14), for a realistic system. While there is plenty of them, let us focus on quantum systems at room temperature, condensed-matter systems, low-energy nuclear systems, and the unitary Fermi gas, for which a nonrelativistic quantum description is applicable.

For a condensed-matter system at room temperature,

$$\lambda_{\text{MSS}}^{\text{CM}} = \frac{\pi T}{\hbar} \approx 1.2 \times 10^{14} \text{ s}^{-1}, \quad (22)$$

and combining this with the time it takes, an electron with a kinetic energy of 3 eV to traverse 100 nm ( $\tau_{\text{cross}} = 1.3 \times 10^{-13}$  s), we obtain

$$\lambda_{\text{MSS}}^{\text{CM}} \tau_{\text{cross}} \approx 15. \quad (23)$$

We used 100 nm as the possible size of a quantum billiard, which is also a reasonable estimate of the mean-free path in typical metals.

A characteristic temperature of an excited nucleus is  $T = O(1)$  MeV, which leads to

$$\lambda_{\text{MSS}}^{\text{nuclear}} \approx 0.016 \text{ c/fm} = 5.33 \times 10^{-26} \text{ s}^{-1}. \quad (24)$$

A heavy nucleus has a diameter  $\approx 12$  fm, a nucleon has a velocity  $\approx c/4$ , and the time it takes to cross a nucleus is  $\tau_{\text{cross}} \approx 50 \text{ fm}/c$ , so

$$\lambda_{\text{MSS}}^{\text{nuclear}} \tau_{\text{cross}} = O(1). \quad (25)$$

The time between two nucleon collisions is not much different,  $\tau_{\text{coll}} \approx \tau_{\text{cross}}$ .

Another system to which we turn our attention to is the unitary Fermi gas (UFG), which is the ‘‘most superfluid system’’ known, with a critical temperature  $T_c \approx 0.17\varepsilon_F$ , where  $\varepsilon_F = \hbar^2 k_F^2/2m$  is the Fermi energy of the noninteracting Fermi gas with the same number density  $n = k_F^3/3\pi^2$ . For the UFG the two-body collision time is  $t_{\text{coll}} \approx \pi \hbar/2\varepsilon_F$  and thus at  $T_c$ ,

$$\lambda_{\text{MSS}}^{\text{UFG}} t_{\text{coll}} = O(1), \quad (26)$$

and thus is similar to the estimates obtained above.

In all these cases, the estimates of  $\lambda$  given by Eq. (14) are upper-bound estimates and one would expect, according to Eq. (18),

$$\lambda_{\text{MSS}} \tau_{\text{equil}} \ll 1 \quad (27)$$

in order to observe chaotic behavior in a quantum system in statistical equilibrium. The question arises as to whether such strongly interacting nonrelativistic fermions could be chaotic in reality. The times  $\tau_{\text{coll}}$  and  $\tau_{\text{cross}}$  are referred to as dissipation and scrambling times, respectively, in Ref. [20] and related studies. What our estimates here show is that, in physical systems of interest in condensed matter, nuclear, and cold atom physics, there is no separation of scales between the dissipation and scrambling times and the conjectured onset of the chaoticity timescale  $1/\lambda_{\text{MSS}}$ .

### B. Time-dependent density-functional theory

Nevertheless, the initial question we raised is still legitimate: Do the Schrödinger and DFT descriptions, which are identical for one-body observables, display any chaoticity? This issue, which was not addressed in the literature yet, specifically for time-dependent phenomena, except for a few instances we are aware of [39–42]. In particular, Balian and Vénéroni [39] address a narrower question concerning the Lyapunov stability of the time-dependent Hartree-Fock (TDHF) approximation and of the random-phase approximation (RPA) only in the case when the initial state minimizes either the microcanonical, canonical, or the grand canonical partition function, respectively. Since at the minimum of a partition function the RPA spectrum is real [43], a Lyapunov instability is naturally not expected and formally it follows to be a mathematically correct statement [39], for either a classical or a quantum many-body system. Our interest here is the more general problem, when the initial state of the quantum system is a (highly) excited state.

DFT does not provide a recipe to construct the energy density functional and thus any DFT implementation relies on a number of assumptions. Even in the case of electrons in

atoms and molecules or in condensed-matter systems, even though the Coulomb interaction is known and the nonrelativistic Schrödinger equation is very accurate in principle for their description. For nuclear systems the situation is even worse, since the interaction between nucleons is not known with enough accuracy, and moreover the relativistic effects are not entirely negligible and the effects of non-nucleon degrees of freedom (virtual mesons, quarks, and gluons) are sometimes required. Nevertheless, as in the case of the Schrödinger equation, where we know the form of the equation and have to provide the interparticle interaction, in the case of DFT we know the framework and we have to provide the energy density functional.

In 1964, Hohenberg and Kohn [32] proved the remarkable mathematical theorem that the many-electron wave function of an  $N$ -electron system in the presence of nuclei is in one-to-one correspondence with the electron number density. This result implies that the  $N$ -electron wave function is fully determined by the electron number density alone. It also implies that an energy density functional depending on the electron number density exists, and its minimum determines the ground-state electron number density and the ground-state energy of the  $N$ -electron system, in full agreement with the solution of the  $N$ -electron Schrödinger equation. This theorem has been generalized over the years to any excited state, to electron systems in various statistical ensembles, and to time-dependent phenomena [36–38]. Since the specific form of the Coulomb electron-electron interaction plays no role in these proofs, these results apply equally to any many-fermion systems, irrespective of the nature of the (static) interaction between them. One should remember also that DFT does not provide information about the  $n$ -body number densities for  $n > 1$ . If the energy density functional is known then one can extract only the one-body number density, the energy of the system, and related observables.

A particular many-fermion system deserves special attention: the unitary Fermi gas (UFG) suggested by Bertsch [44–46]. In the Bertsch [44] formulation, the UFG is a homogeneous infinite system of equal number of spin-up and spin-down fermions, interacting with a zero-range potential and an infinite scattering amplitude. The UFG energy per particle of a large homogeneous  $N$ -particle system is then given by the function

$$\lim_{a \rightarrow \infty} \lim_{r_0 \rightarrow 0} \frac{E(N, V, \hbar, m, r_0, a)}{N} \Big|_{\frac{N}{V} = \text{const}} = \xi \frac{3}{5} \varepsilon_F, \quad (28)$$

$$n = \frac{N}{V} = \frac{k_F^3}{3\pi^2}, \quad \varepsilon_F = \frac{\hbar^2 k_F^2}{2m}, \quad (29)$$

where  $V$ ,  $a$ ,  $r_0$ , and  $m$  are the volume, scattering length, effective range, and mass of the fermions, respectively, and  $n$ ,  $k_F$ , and  $\varepsilon_F$  are the number density, Fermi wave vector, and Fermi energy of the free Fermi gas, respectively, with the same  $N$  and  $V$ . For the UFG, apart from mass  $m$  and Planck’s constant [which factors out in Eq. (28)], the only dimensional system-dependent quantity is the Fermi wave vector. The dimensionless constant  $\xi$  is known as the Bertsch parameter, and by now has been determined both theoretically  $\xi = 0.372(5)$  [47] and experimentally  $\xi = 0.376(5)$

[48]. From dimensional arguments and requiring translational, rotational, time-reversal symmetries, the Galilean invariance, and the renormalizability of the theory one can show that, for an inhomogeneous system, the energy density functional of a UFG is determined as

$$\varepsilon(\mathbf{r}) = \frac{\hbar^2}{m} \left[ \alpha \frac{\tau(\mathbf{r})}{2} + \beta \frac{3(3\pi^2)^{2/3} n^{5/3}(\mathbf{r})}{5} + \gamma \frac{|v(\mathbf{r})|^2}{n^{1/3}(\mathbf{r})} - (\alpha - 1) \frac{j^2(\mathbf{r})}{n(\mathbf{r})} \right] + \dots, \quad (30)$$

where we have neglected further gradient corrections like  $\approx |\nabla n|^2/n$ . The number, kinetic, anomalous, and current densities are defined as follows:

$$n(\mathbf{r}) = 2 \sum_{0 < E_k < E_c} |v_k(\mathbf{r})|^2, \quad (31)$$

$$\tau(\mathbf{r}) = 2 \sum_{0 < E_k < E_c} |\nabla v_k(\mathbf{r})|^2, \quad (32)$$

$$v(\mathbf{r}) = \sum_{0 < E_k < E_c} u_k(\mathbf{r}) v_k^*(\mathbf{r}), \quad (33)$$

$$j(\mathbf{r}) = 2 \text{Im} \sum_{0 < E_k < E_c} v_k^*(\mathbf{r}) \nabla v(\mathbf{r}). \quad (34)$$

They are parametrized in terms of the Bogoliubov quasi-particle wave functions (qpwf)  $u_k(\mathbf{r})$ ,  $v_k(\mathbf{r})$ , obtained as the solutions of the self-consistent equations

$$\begin{pmatrix} (h(\mathbf{r}) - \mu) & \Delta(\mathbf{r}) \\ \Delta^*(\mathbf{r}) & -(h^*(\mathbf{r}) - \mu) \end{pmatrix} \begin{pmatrix} u_k(\mathbf{r}) \\ v_k(\mathbf{r}) \end{pmatrix} = E_k \begin{pmatrix} u_k(\mathbf{r}) \\ v_k(\mathbf{r}) \end{pmatrix}, \quad (35)$$

where

$$h(\mathbf{r}) = -\frac{\hbar^2 \alpha}{2m} \nabla^2 + \frac{\delta \varepsilon(\mathbf{r})}{\delta n(\mathbf{r})} + V_{\text{ext}}(\mathbf{r}), \quad \Delta(\mathbf{r}) = -\frac{\delta \varepsilon(\mathbf{r})}{\delta v^*(\mathbf{r})}. \quad (36)$$

Here  $V_{\text{ext}}(\mathbf{r})$  stands for a trapping potential and  $\mu$  is the chemical potential. The need for the kinetic-energy density in addition to the number density was discussed in Ref. [33]. The anomalous and current densities are required to be able to disentangle the superfluid phase from the normal phase and the static system from the system with flow, respectively. The current density is needed in the case of currents, e.g., when quantized vortices are present. The dimensionless parameters  $\alpha$ ,  $\beta$ , and  $\gamma$  are extracted from quantum Monte Carlo calculations of the homogeneous UFG [49,50].

Many properties of trapped inhomogeneous finite UFG can at this point be evaluated by using the two different, independent, and exact methods, the DFT and the solution of the many-body Schrödinger equation using a Monte Carlo approach (QMC). The DFT and QMC results agree to the level of QMC numerical errors [49,50], and therefore the DFT and Schrödinger descriptions indeed agree as expected.

The time-dependent systems are described within the TDDFT framework,

$$i\hbar \begin{pmatrix} \dot{u}_k(\mathbf{r}, t) \\ \dot{v}_k(\mathbf{r}, t) \end{pmatrix} = \begin{pmatrix} [h(\mathbf{r}, t) - \mu] & \Delta(\mathbf{r}, t) \\ \Delta^*(\mathbf{r}, t) & -[h^*(\mathbf{r}, t) - \mu] \end{pmatrix} \times \begin{pmatrix} u_k(\mathbf{r}, t) \\ v_k(\mathbf{r}, t) \end{pmatrix}. \quad (37)$$

A direct comparison of the time-dependent Schrödinger and TDDFT solutions has not yet been performed. However, the time-dependent Schrödinger equation for a simplified  $N$ -fermion superfluid system, very similar to the UFG [51–53] has similar solutions with the TDDFT for UFG [54]. One of the most spectacular successes of TDDFT was the correct identification of the generation of vortex rings and their dynamics [55–58], which were initially incorrectly identified as heavy solitons [59] and later confirmed as vortex rings experimentally as well [60]. Subsequently, it was demonstrated that the TDDFT for the unitary Fermi gas correctly describes the evolution of the full solitonic cascade, contrary to simplified approaches like the standardly applied Gross–Pitaevskii equation [58].

We discuss two other examples of strongly interacting many-fermion systems: nuclear fission and collisions of superfluid heavy ions. In the case of nuclear systems, we have so far only approximate forms of the energy density functionals, which are also significantly more complex than the UFG energy density functional. To describe nuclear systems one has to explicitly add neutron and proton degrees of freedom and also the spin-orbit interaction and the corresponding number spin densities, for details, see Refs. [61–67]. The nuclear qpwf, separately for neutrons and protons, have four components  $\{u_k(\mathbf{r}, \uparrow), u_k(\mathbf{r}, \downarrow), v_k(\mathbf{r}, \uparrow), v_k(\mathbf{r}, \downarrow)\}$  to account for spin 1/2 in the presence of the spin-orbit interaction.

Since both the Schrödinger equation and the TDDFT lead, in principle, to the same number density  $n(\mathbf{r}, t)$  and related observables, it is natural to examine the sensitivity to initial conditions of this quantity. We introduce noise in the initial state according to the prescription discussed in Ref. [42]. Namely, in the case of UFG, we slightly alter the initial values of the qpwf as follows:

$$\begin{pmatrix} u_k(\mathbf{r}, 0) \\ v_k(\mathbf{r}, 0) \end{pmatrix} \rightarrow \begin{pmatrix} u_k(\mathbf{r}, 0)[1 + \epsilon \alpha_u(\mathbf{r})] \\ v_k(\mathbf{r}, 0)[1 + \epsilon \alpha_v(\mathbf{r})] \end{pmatrix}, \quad (38)$$

where  $\epsilon$  is the strength of the noise and  $\alpha_{u,v}(\mathbf{r})$  are complex numbers with real and imaginary uniform random numbers in the interval  $[-1, 1]$ . The random quantity  $\alpha(\mathbf{r})$  appear to introduce discontinuities in the modified qpwf, as neighboring lattice points are not correlated. However, this apparent discontinuity is at the scale  $p_{\text{cut}} = \hbar\pi/l$ , where  $l$  is the lattice constant, and thus accommodated in our numerical scheme. In the case of nuclear systems, all four components of the proton and neutron qpwf are modified accordingly. The perturbed qpwf are not orthonormal anymore, but the solutions of the corresponding TDDFT equations satisfy all expected symmetries and conservation laws. According to our discussion in Sec. II, this type of perturbation of the initial qpwf is equivalent to the change in coordinates and momenta when studying the sensitivity to initial conditions in the equivalent classical

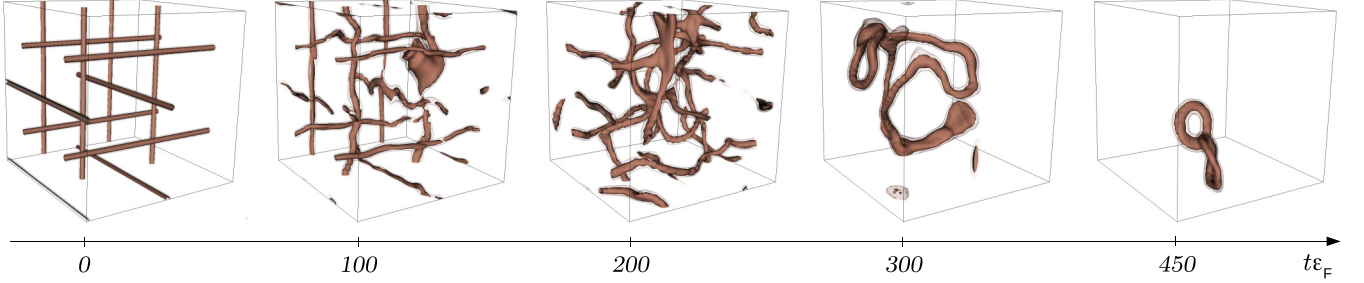


FIG. 1. Several consecutive frames demonstrating the evolution of a system with 12 quantized vortices, perturbed by a spherical ball stirring them in the time interval  $\Delta t = 170\epsilon_F^{-1}$ , after which the UFG is left to evolve undisturbed. The system remains superfluid during the entire evolution. Time is in units of  $1/\epsilon_F$  and in the case of UFG one also typically chooses  $\hbar = 1$ .

Hamiltonian framework of either the Schrödinger equation or of the corresponding TDDFT. Since the primary DFT theorem implies that there is a one-to-one mapping  $\Psi \leftrightarrow n$ , we can alternatively apply the perturbation to the densities. The specific method of introducing the perturbation should not influence the final result.

### C. Vortex dynamics in a unitary Fermi gas

The first example that we discuss is the simulation of the dynamics of 12 quantized vortices in a UFG with  $N = 1004$  fermions in a simulation box  $N = N_x N_y N_z = 40^3$ , where the dimension of the equivalent classical phase space is  $4 \times N^2 \approx 1.6 \times 10^{10}$ . Initially, the vortices are parallel to the sides of the simulation box and have alternate vorticities, see the first frame in Fig. 1. At time  $t = 0$  a spherical ball is introduced into the system and starts stirring the system until the time  $t = 170\epsilon_F^{-1}$  when the ball is again extracted (in the case of an UFG, one uses the units  $m = \hbar = 1$ ) and during this time energy is pumped into the system. The UFG is superfluid initially, and the amount of energy pumped into the system during the time interval  $(0, 170)\epsilon_F^{-1}$  is sufficiently small so that the system remains superfluid. The stirring process destabilizes the vortex grid and vortices begin to cross and reconnect, as conjectured by Feynman [68], and in this manner quantum turbulence (QT) is generated. This type of turbulence is routinely characterized as a random and chaotic motion of the fluid. Indeed, most of studies in the QT field are done by means of the so-called vortex filament model (VFM), which converts the quantum problem into classical motion of vortex lines that interact nonlinearly [69]. Since the number of vortices and antivortices are equal, eventually they annihilate each other and after  $t \approx 600\epsilon_F^{-1}$  there are no vortices left in the system.

The density plays the central role in the DFT approach, and in order to measure the Lyapunov exponent we will track this quantity. In Fig. 2 we show as a function of time

$$\frac{\lambda(t)}{\epsilon_F} = \frac{1}{2\epsilon_F t} \ln \frac{\int d^3 r [n_\epsilon(\mathbf{r}, t) - n_0(\mathbf{r}, t)]^2}{\int d^3 r [n_\epsilon(\mathbf{r}, 0) - n_0(\mathbf{r}, 0)]^2}, \quad (39)$$

where  $n_\epsilon(\mathbf{r}, t)$  and  $n_0(\mathbf{r}, t)$  are the densities arising from perturbed and unperturbed initial states, respectively. These results were obtained using the code [70]. We used different methods to introduce the initial perturbation. Noise in the

initial qpwf's, in the form of Eq. (38), of different strengths ( $\epsilon = 0.5\%$ , and  $1\%$ ) provide a very similar value of  $\lambda(t)$  for late times. Alternatively, instead of perturbing the wave functions, one can perturb the initial Hamiltonian by adding the noise to the density or to the order parameter, however, we do not find significant sensitivity of the final result on the perturbation method. Finally, we have checked that the result does not depend on the discretization. Compare the time series for spatial lattices  $40^3$  and  $32^3$ , where we keep a fixed volume of the simulation domain and adjusted the lattice spacing accordingly. All these result clearly demonstrate that for the studied system the Lyapunov exponent  $\lambda_{\text{UFG}} = \lim_{t \rightarrow \infty} \lambda(t) \approx 0.005\epsilon_F$ .

At times larger than  $t \approx 600\epsilon_F^{-1}$  the vortices disappeared from the system, the system becomes a uniform gas with many excited phonons and the time average is a thermal equilibrium state. From the energy in the final state, using the equation of state  $E(T)$ , which was obtained quite accurately both theoret-

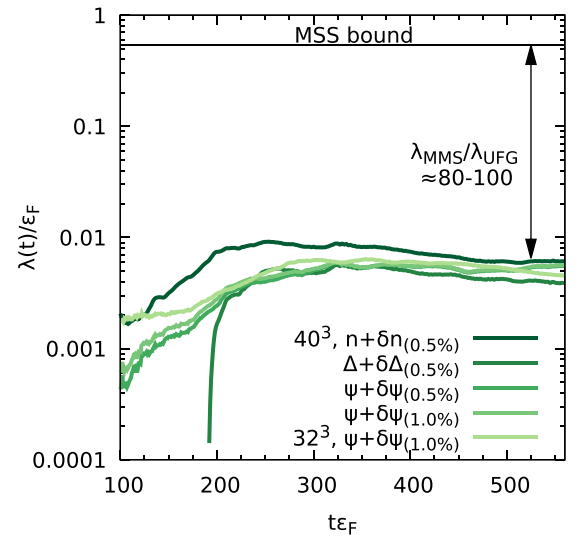


FIG. 2. The time evolution of  $\lambda(t)$  for different methods of introducing the noise: perturbation of quasiparticle wave functions ( $\Psi + \delta\Psi$ ), and initial Hamiltonian through density ( $n + \delta n$ ) or the order parameter ( $\Delta + \delta\Delta$ ). The value after label (0.5% or 1.0%) indicates strength of the noise  $\epsilon$ . On top the upper bound by Maldacena *et al.* [20] is depicted.

ically and experimentally [46], we determine the temperature  $T$  corresponding to the equilibrated state,  $T/\varepsilon_F \approx 0.17$ , which is practically equal to the critical temperature  $T_c$ . The length of simulations are, however, rather short for the system to have thermalized. At thermal equilibrium at this temperature the UFG is most likely in the so-called pseudogap phase, when the long-range superfluid correlations vanished, but a pairing gap is still present [71–75] and where the ratio of the viscosity to the entropy is minimal [76], and the system is often referred to as a perfect fluid. At this temperature, evaluated using the UFG equation of state [77–79],

$$\frac{\lambda_{\text{MSS}}^{\text{UFG}}}{\varepsilon_F} = \frac{\pi T}{\varepsilon_F} \approx 0.53, \quad (40)$$

which is about two orders of magnitude higher than what we observe in our calculations.

#### D. Nuclear fission

In Ref. [42] we reported preliminary results on the influence of noise in initial conditions in TDDFT simulations on some properties of the emerging nuclear reaction products. In such calculations, the reaction products are followed in time only until they are reasonably far spatially separated and they do not exchange energy, momentum, or particles anymore. At that point the various properties of the emerging reaction products are evaluated, and that is where we judge the sensitivity to the initial conditions.

TDDFT nuclear fission simulations are equivalent to a classical Hamiltonian system with a dimension of the phase space  $(4 \times 30^2 \times 60)^2 \approx 4.7 \times 10^{10}$  and we notice that the maximum Lyapunov exponent is very small or vanishing. In Fig. 3 we plot the quantity

$$\lambda(t) = \frac{1}{2t} \ln \frac{\int d^3r [n_\epsilon(\mathbf{r}, t) - n_0(\mathbf{r}, t)]^2}{\int d^3r [n_\epsilon(\mathbf{r}, 0) - n_0(\mathbf{r}, 0)]^2}. \quad (41)$$

It is clear that the Lyapunov exponent again is very small, well below the conjectured upper limit  $\lambda_{\text{MSS}}^{\text{nuclear}}$ , see Eq. (24). Here, we restrict ourselves only to perturbations of initial quasiparticle wave functions of the type given in Eq. (38). We start the induced fission simulation relatively late in the evolution of the reaction  $^{235}\text{U}(n, f)$  [80]. As has been well known for many decades, when a low-energy neutron is absorbed by a nucleus, a compound nucleus is formed [81], which lives for a very long time  $\approx 10^{-15}$  s. before scission. At this excitation energy the level density is very high [28],

$$\rho(E) \propto \exp(\sqrt{aE}), \quad \text{where } a \propto A, \quad (42)$$

and  $A$  is the atomic number. During this time the shape of the compound nucleus changes very slowly from a very compact almost spherical one to one resembling a peanut at the top of the outer fission barrier. During this time the dynamics of the nucleus is qualitatively similar to a biological cell division [82], in which the nuclear surface tension competes with the Coulomb interaction, leading ultimately to nuclear scission [82].

From the top of the outer fission barrier until scission the nuclear shape evolves relatively fast  $\approx 10^{-19}$  s. This time is, however, much longer than the characteristic single-particle

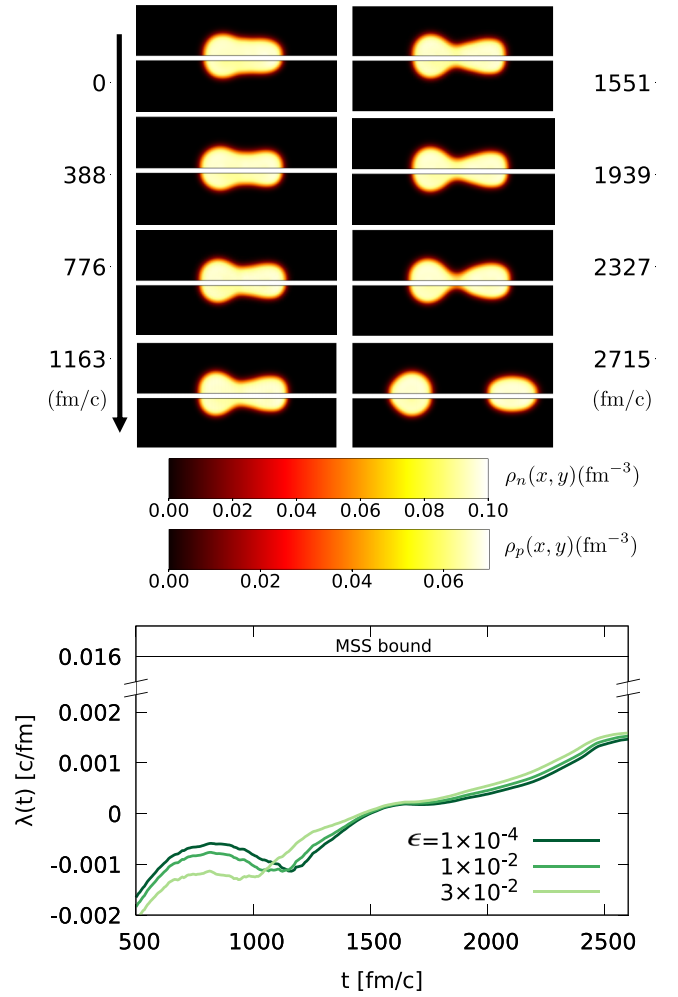


FIG. 3. In the upper panel we display the evolution of the neutron (upper half of each frame) and proton (lower half of each frame) number densities of fissioning  $^{236}\text{U}$  in a simulation box  $30^3 \times 60 \text{ fm}^3$  into a heavy (left) and light (right) fragments. The neutron and proton numbers of the heavy (left) and of the light (right) fragments are (83.6, 52.2) and (60.4, 39.8), respectively. The shapes of the distributions and the neutron and proton numbers of the fission fragments are hardly affected by the level of noise level. In the lower panel we show the time evolution of  $\lambda(t)$  as obtained from Eq. (41). After scission, which occurs at  $t \approx 2400 \text{ fm/c}$ , the excited fission fragments emerge, after thermalization, with temperatures  $T \approx 1 \text{ MeV}$  [41,63], which results in  $\lambda_{\text{MSS}}^{\text{nuclear}} \approx 0.016 \text{ c/fm}$ .

time  $\approx 10^{-22}$  s. Nucleons collide with the moving walls of the fissioning nucleus, the nucleus heats up, its intrinsic entropy increases, similar to Fermi’s acceleration mechanism for the origin of cosmic radiation [83]. The nuclear dynamics is highly nonequilibrium [63,66,67] and the collective or the nuclear shape motion of the fissioning nuclear system is overdamped.

The dynamics of the fissioning nucleus from the outer fission barrier until scission is similar to some extent to the evolution of a complex molecule, which undergoes some big rearrangements of its atoms. The total energy is conserved, but energy is continuously converted from the nuclear configura-



tional energy in the molecule into the energy of the electron cloud. In the case of the fissioning nucleus, the configuration energy is approximately equal to the sum of the Coulomb energy and the surface energy. While the nucleus evolves from the outer fission barrier towards the scission configuration it elongates, while preserving its volume. The surface area increases and the surface energy increases proportionally, but at the same time the average separation of the electric charges increases and the Coulomb energy decreases. At small elongations of the fissioning nucleus the surface potential energy dominates, but as soon as the nucleus reaches the outer fission barrier the sum of surface and Coulomb energies is dominated by the Coulomb energy [82]. The approximate sum of the surface potential and Coulomb energy decreases by  $\approx 15\text{--}20$  MeV from the top of the fission barrier until scission. This energy difference is converted into internal energy of the system. Only a small part ( $\approx 10\%$ ) of the energy is converted into kinetic flow energy of the nuclear fluid, the rest being converted into heat.

The other noticeable aspect of the fission dynamics from the outer fission barrier until scission put in evidence in TDDFT simulations is that, during the descent from the neighborhood of the outer fission barrier, the shape dynamics has a focusing character. Since the shape evolution is overdamped the collective motion is similar to that of a parachute, which follows the steepest descent with a rather small “terminal velocity.” As a result, trajectories with rather distinct initial conditions behave like a group of parachutists who jump out of a plane at different times and land relatively close to each other, as both their vertical and longitudinal velocities are damped. This is the reason why the  $\lambda(t)$  in the case of fission is negative before the scission occurs.

Note that, after the scission, the number of nucleons in each fragment, as well as their energies, are fixed. Since these are measured observables experimentally, this moment defines for all practical purposes the meaning of the “infinite-time limit.” In spite of the complex nature of the problem, the evolution turns out to be very weakly sensitive to the initial noise, with the corresponding Lyapunov exponent being well below the prediction of Maldacena *et al.* [20].

### E. Collisions of heavy ions

A second nuclear physics example is from heavy-ion collisions  $^{238}\text{U} + ^{238}\text{U}$  at a center-of-mass energy of 1200 MeV. In this case the dimension of the equivalent phase space is  $(4 \times 30^3 \times 64)^2 \approx 5.3 \times 10^{10}$ . After the collision, the two fragments are highly excited because the final total kinetic energy is only  $\approx 600$  MeV. By changing the initial kinetic energy from 600 to 1600 MeV the final kinetic energy barely changes, and the final estimated temperatures of the fragments varies by at most a factor of two. The case illustrated in Fig. 4 is in the middle of this energy range, see also Ref. [42]. From the excitation energy of the reaction fragments one can extract their equilibrium temperatures  $T \approx 3.5$  MeV, obtained using Bethe formula [28,42], which according to Eq. (14) leads to an upper limit  $\lambda_{\text{MSS}} = 0.057$  c/fm.

Upon adding noise at the level  $\epsilon = 0.03$ , see Eq. (38), the nuclei acquire a total initial excitation energy of about

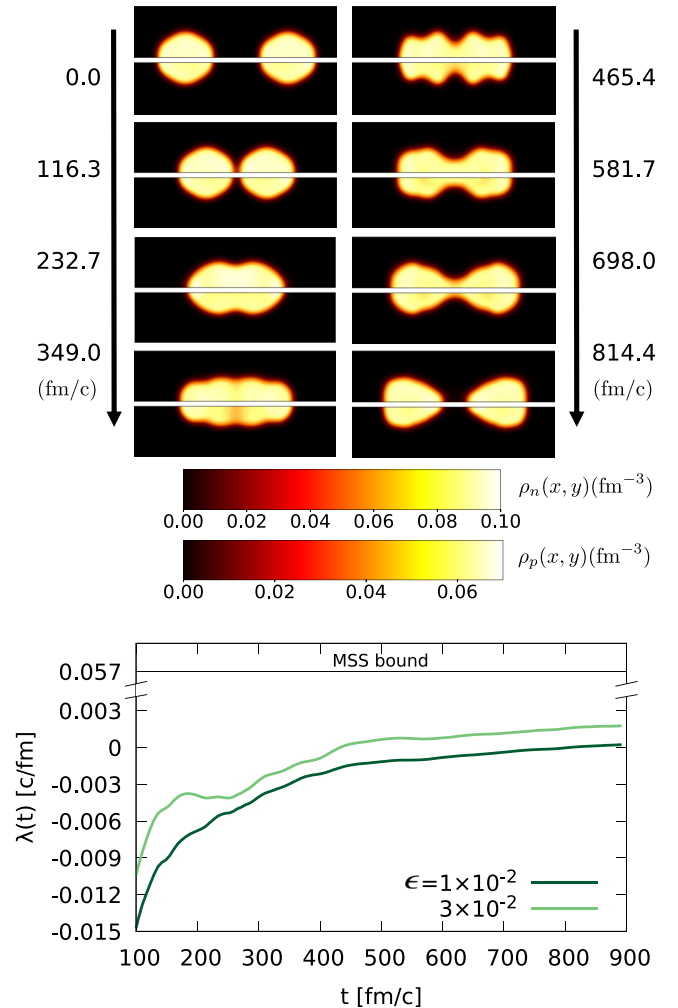


FIG. 4. In the upper panel we display the evolution of the neutron (upper half of each frame) and proton (lower half of each frame) number densities of a fissioning  $^{238}\text{U} + ^{238}\text{U}$  collision in a simulation box  $30^3 \times 64$  fm<sup>3</sup> into two highly excited and not yet equilibrated fragments. The shapes of the neutron and proton distributions are hardly affected by the noise level. In the lower panel, the time evolution of  $\lambda(t)$ , Eq. (41), in the case collision of two heavy ions  $^{238}\text{U} + ^{238}\text{U}$  at a center-of-mass energy of 1200 MeV is shown. After separation the excited fragments emerge, after thermalization, with temperatures  $T = 3.55$  MeV, which results in a  $\lambda_{\text{MSS}}^{\text{nuclear}} \approx 0.057$  c/fm.

50 MeV, corresponding to an initial temperature  $T \approx 1.5$  MeV. In a time  $\approx 250$  fm/c the two nuclei touch “noses” and remain in contact up to a time  $\approx 700$  fm/c. Until the nuclei coalesce, which a relatively fast process, only the long-range Coulomb interaction between them leads a small charge polarization of the colliding nuclei. The two nuclei form a dinucleus at about 300 fm/c, which starts separating into two fragments around 550 fm/c and the contact time is thus relatively short. Similarly to the fission process, after the separation, fragments and their properties are fixed, and there is no reason to consider the evolution in the context of extracting of the Lyapunov exponent. Nevertheless,  $\lambda(t)$  appears to be

almost saturated, and again by about two orders of magnitude less than the upper bound.

#### IV. CONCLUSIONS

We have analyzed several strongly interacting quantum many-fermion systems in which superfluid correlations are very important in order to correctly describe their nonequilibrium dynamics, with a number of degrees of freedom of the order of  $10^{10}$  or larger. Their dynamical evolution is described within an extension of the TDDFT to superfluid systems, which is expected to be mathematically equivalent to the description of the same systems using the time-dependent many-body Schrödinger equation, but only at the level of the one-body densities. Since the Schrödinger equation is linear, no exponential sensitivity to the variations of the initial conditions exists. Therefore, if one replaces the initial many-body wave function  $\Psi(x_1, \dots, x_N, t) \rightarrow \Psi(x_1, \dots, x_N, 0) + \delta\Psi(x_1, \dots, x_N, 0)$

$$\langle \Psi(0) | \delta\Psi(0) \rangle \equiv \langle \Psi(t) | \delta\Psi(t) \rangle \ll 1, \quad (43)$$

one does not expect an exponential divergence of the two wave functions. The overlap of two arbitrary wave functions  $\langle \Psi_1(0) | \Psi_2(0) \rangle = \langle \Psi_1(t) | \Psi_2(t) \rangle$  is always preserved in the case of a time-dependent Schrödinger equation. As we mentioned in the introduction, the Schrödinger equation is also mathematically equivalent to a system of classical coupled harmonic oscillators, for which the absence of chaos is well known.

Even though the Schrödinger description is in principle mathematically identical to the DFT description at the one-body density level, the DFT equations are nonlinear, their sensitivity, or the absence of such sensitivity, to the initial conditions has never been demonstrated. In this study we have presented strong arguments that for very large realistic quantum many-body systems the Lyapunov exponents within a DFT description are much smaller than the conjectured by Maldacena *et al.* [20] upper limit. However, even though the Lyapunov exponents are nonvanishing, they are small enough as not to alter the quality of the conclusions inferred within the present TDDFT framework.

We presented typical simulation results for three different strongly interacting many-fermion superfluid systems. By changing various parameters, particle number, energy density functionals, energy of the system, and so forth, the results remain qualitatively similar. In all cases the Lyapunov exponents are smaller by a factor of 10,  $\dots$ , 100 than the upper limit conjectured by Maldacena *et al.* [20], Tsuji *et al.* [21], but likely not vanishing as one would have expected, if the TDDFT is mathematically equivalent to the Schrödinger equation at the level of one-body number density. The most obvious offender appears to be the energy density functional used. Strictly speaking, in the TDDFT the evolution equations are expected to have memory terms [37,38], which are absent in all the cases we have discussed here. If the quantum evolution is “slow” one can invoke the adiabatic limit of the energy density functional, when the memory terms can be susceptibly neglected, which was assumed in all the cases we studied. Thus, the measure to what extent the Lyapunov

exponents are not vanishing points to the accuracy to the current implementation of the TDDFT formalism in the case of strongly interacting fermion systems.

A second cause leading to nonvanishing Lyapunov exponents, which we cannot fully rule out at this time, could be due to the accumulation of numerical errors in evaluating the evolution of a system with  $O(10^{10})$  phase-space variables in current numerical implementations. The tests we have performed so far indicate that our codes are, however, numerically quite accurate [42,70]. On the other hand, the theory is operative only if one can use it to make predictions. It is hard to achieve it without practical implementation. The Nobel Committee already recognized this critical aspect when awarding the prize in 1998 to Walter Kohn “for his development of the density-functional theory.” Thus, in reality, one should measure the quality of the TDDFT by taking into account contributions to the Lyapunov exponent coming from both sources: the accuracy of the underlying energy density functional and its numerical realization.

The absence of positive Lyapunov exponents within TDDFT is crucial when one considers extracting the magnitude of fluctuations of various physical quantities within a mean-field approach [84–90], such as neutron, proton, and neutron-proton particle variances. Balian and Vénéroni [84] designed a variational approach based on an action-like functional

$$\mathcal{I} = \text{Tr} \mathcal{A}(t_1) \mathcal{D}(t_1) - \int_{t_0}^{t_1} dt \text{Tr} \left( \mathcal{A}(t) \frac{d\mathcal{D}(t)}{dt} + i[H, \mathcal{D}(t)] \right), \quad (44)$$

where  $\mathcal{D}(t)$  and  $\mathcal{A}(t)$  are two time-dependent operators of the same nature as a density operator and an observable, and  $H$  is the Hamiltonian. Unfortunately, this action-like functional cannot be minimized and can only be made stationary with respect to arbitrary variations of both  $\mathcal{D}(t)$  and  $\mathcal{A}(t)$ , subject to boundary conditions

$$\mathcal{D}(t_0) = D, \quad \mathcal{A}(t_1) = A, \quad (45)$$

where  $D$  is the initial value of the density matrix and  $A$  is the final value of the observable of interest. This approach appears to be useful in practice in carefully chosen situations. The dispersion of the observable  $\mathcal{A}(t_1)$  can then be determined from the limit

$$\langle \langle \mathcal{A}^2(t_1) \rangle \rangle = \frac{1}{2} \lim_{\epsilon \rightarrow 0} \frac{\langle [D - \sigma(t_0, \epsilon)]^2 \rangle}{\epsilon^2}, \quad (46)$$

where

$$\sigma(t_1, \epsilon) = \mathcal{A}(t_1, \epsilon) = e^{i\epsilon A} \mathcal{D}(t_1) e^{-i\epsilon A}, \quad (47)$$

where one chooses in practice  $\epsilon = 0.001, \dots, 0.0001$ . One thus needs to propagate the equations of motion forward in time for  $\mathcal{D}(t)$  and backward in time for  $\sigma(t, \epsilon)$ , and in the presence of chaoticity such results will become totally unpredictable. As we have shown here and partially in Ref. [42] the TDDFT equations lack sensitivity to initial conditions with high numerical accuracy.

For practical reasons, the resilience of the TDDFT framework to describe the evolution of dense quantum many-body

systems with respect to the level of noise is remarkable. On the other hand, the present results show a different aspect of the decades old question: Under what conditions can we observe the sensitivity to initial conditions in realistic time-dependent nonequilibrium phenomena in dense quantum many-body systems in the absence of the limit  $\hbar \rightarrow 0$ ? In TDDFT applications it makes sense to examine the validity of the theory up to the point in time when predictions are expected. In the case of quantum turbulence at the stage when the quantized vortices have already decayed, in the case of nuclear fission and heavy-ion collisions in nuclear physics that is at the time when the properties of the emerging fragments have been defined. These timescales are to some extent not very long, but large enough to allow for the evidence of sensitivity to initial conditions. Niels Bohr's compound nucleus [81], formed for example in the case of the neutron-induced fission of  $^{235}\text{U}(n, f)$  [80], is an example of a quantum many-fermion system which evolves for extremely long times  $\tau \approx 10^{-15}$  s. To have a noticeable effect of the sensitivity to initial conditions in a compound nucleus one would have to distinguish or measure properties of different quantum states, characterized by different quantum numbers, thus be sensitive to energy differences comparable to the average level separation  $\Delta E = 1/\rho(E)$ . One could argue also that one would have to discriminate between systems with spectral properties characterized either of the random matrix theory—typically the Gaussian orthogonal ensemble (GOE)—or of the integrable or Poisson type [12–14, 16–19, 29, 30, 91], in order to distinguish between various final configurations, thus be able to probe

energy differences larger than the separation between several levels in complex quantum systems at significant excitation energies, where the level density is quite high. Induced fission [80], one of the three cases we considered here, is an example where a compound nucleus is formed [81], at an excitation energy with very high level density [28], and the outcomes of the reaction are largely independent of the excitation mechanism. Such long timescales are likely unachievable within an unrestricted real-time quantum framework and using present and near future computational resources.

## ACKNOWLEDGMENTS

A.B. thanks V. Zelevinsky for reading the initial draft of the paper and for a number of comments. A.B. was supported by U.S. Department of Energy, Office of Science, Grant No. DE-FG02-97ER41014 and in part by NNSA cooperative Agreement DE-NA0003841. The work of I.A. is based upon work supported by the Department of Energy, National Nuclear Security Administration, under Award Number DE-NA0003841. The G.W. work was supported by the Polish National Science Center (NCN) under Contracts No. UMO-2017/26/E/ST3/00428. This research used resources of the Oak Ridge Leadership Computing Facility, which is a U.S. DOE Office of Science User Facility supported under Contract No. DE-AC05-00OR22725 and of the National Energy Research Scientific computing Center, which is supported by the Office of Science of the U.S. Department of Energy under Contract No. DE-AC02-05CH11231.

- 
- [1] H. Poincaré, Sur le problème de trois corps et les équation de la dynamique, *Acta Math.* **13**, 1 (1890).
- [2] M. Rågstedt, From order to chaos: the prize competition in honor of King Oscar II, <http://www.mittag-leffler.se/library/henri-poincare>.
- [3] A. M. Lyapunov, The general problem of stability of motion, *Int. J. Control* **55**, 531 (1992).
- [4] E. N. Lorenz, Deterministic nonperiodic flow, *J. Atmos. Sci.* **20**, 130 (1963).
- [5] B. Kol, Flux-based statistical prediction of three-body outcomes, *Celest. Mech. Dyn. Astron.* **133**, 17 (2021).
- [6] V. Manwadkar, A. A. Trani, and N. W. C. Leigh, Chaos and Lévy lights in the three-body problem, *Mon. Not. R. Astron. Soc.* **497**, 3694 (2020).
- [7] V. Manwadkar, B. Kol, A. A. Trani, and N. W. C. Leigh, Testing the flux-based statistical prediction of the three-body problem, *MNRAS* **506**, 692 (2021).
- [8] Y. B. Ginat and H. B. Perets, Analytical, Statistical Approximate Solution of Dissipative and Nondissipative Binary-Single Stellar Encounters, *Phys. Rev. X* **11**, 031020 (2021).
- [9] Y. B. Pesin, Characteristic Lyapunov exponents and smooth ergodic theory, *Russ. Math. Surv.* **32**, 55 (1977).
- [10] J. Kaplan and J. Yorke, *Chaotic Behavior of Multidimensional Difference Equations*, edited by H. O. Peitgen and H. O. Walther (Springer, New York, 1979) Vol. Functional Differential Equations and Approximations of Fixed Points.
- [11] L. D. Landau and E. M. Lifshitz, *Fluid Mechanics*, Course of Theoretical Physics (Butterworth-Heinemann, Oxford, 1966), Vol. 6.
- [12] M. L. Mehta, *Random Matrices* (Academic Press, Inc., Boston, 1991).
- [13] O. Bohigas, M. J. Giannoni, and C. Schmit, Characterization of Chaotic Quantum Spectra and Universality of Level Fluctuation Laws, *Phys. Rev. Lett.* **52**, 1 (1984).
- [14] R. Balian and C. Bloch, Solution of the Schrödinger equation in terms of classical path, *Ann. Phys. (NY)* **85**, 514 (1974).
- [15] M. V. Berry and M. Tabor, Closed orbits and the regular bound spectrum, *Proc. Royal Society of London. Series A*, **349**, 101 (1976).
- [16] M. C. Gutzwiller, Periodic orbits and classical quantization condition, *J. Math. Phys.* **12**, 343 (1977).
- [17] M. V. Berry, Quantizing a classically ergodic system: Sinai's billiard and the KKR method, *Ann. Phys. (NY)* **131**, 163 (1981).
- [18] E. J. Heller, Bound-State Eigenfunctions of Classically Chaotic Hamiltonian Systems: Scars of Periodic Orbits, *Phys. Rev. Lett.* **53**, 1515 (1984).
- [19] A. I. Larkin and Y. N. Ovchinnikov, Quasiclassical method in the theory of superconductivity, *J. Exp. Theor. Phys.* **28**, 1200 (1969).
- [20] J. Maldacena, S. H. Shenker, and D. Stanford, A bound on chaos, *J. High Energy Phys.* **08** (2016) 106.
- [21] N. Tsuji, T. Shitara, and M. Ueda, Bound on the exponential growth rate of out-of-time-ordered correlators, *Phys. Rev. E* **98**, 012216 (2018).
- [22] B. Yan, L. Cincio, and W. H. Zurek, Information Scrambling and Loschmidt Echo, *Phys. Rev. Lett.* **124**, 160603 (2020).

- [23] B. Yan and N. A. Sinitsyn, Recovery of Damaged Information and the Out-Of-Time-Ordered Correlators, *Phys. Rev. Lett.* **125**, 040605 (2020).
- [24] L. D. Landau and E. M. Lifshitz, *Statistical Physics, Part I* (Pergamon Press Ltd., Oxford, 1980).
- [25] D. M. Brink, J. Neto, and H. A. Weidenmüller, Transport coefficients for deeply inelastic scattering from the Feynman path integral method, *Phys. Lett. B* **80**, 170 (1979).
- [26] A. Bulgac, G. Do Dang, and D. Kusnezov, Dynamics of a simple quantum system in a complex environment, *Phys. Rev. E* **58**, 196 (1998).
- [27] D. Kusnezov, A. Bulgac, and G. D. Dang, Quantum Lévy Processes and Fractional Kinetics, *Phys. Rev. Lett.* **82**, 1136 (1999).
- [28] H. A. Bethe, An attempt to calculate the number of energy levels of a heavy nucleus, *Phys. Rev.* **50**, 332 (1936).
- [29] J. M. Deutsch, Quantum statistical mechanics in a closed system, *Phys. Rev. A* **43**, 2046 (1991).
- [30] M. Srednicki, Chaos and quantum thermalization, *Phys. Rev. E* **50**, 888 (1994).
- [31] V. Zelevinsky, B. A. Brown, N. Frazier, and M. Horoi, The nuclear shell model as a testing ground for many-body chaos, *Phys. Rep.* **276**, 85 (1996).
- [32] P. Hohenberg and W. Kohn, Inhomogeneous electron gas, *Phys. Rev.* **136**, B864 (1964).
- [33] W. Kohn and L. J. Sham, Self-consistent equations including exchange and correlation effects, *Phys. Rev.* **140**, A1133 (1965).
- [34] E. Runge and E. K. U. Gross, Density-Functional Theory for Time-Dependent Systems, *Phys. Rev. Lett.* **52**, 997 (1984).
- [35] W. Kohn, Nobel Lecture: Electronic structure of matter—wave functions and density functionals, *Rev. Mod. Phys.* **71**, 1253 (1999).
- [36] R. M. Dreizler and E. K. U. Gross, *Density Functional Theory: An Approach to the Quantum Many-Body Problem* (Springer-Verlag, Berlin, 1990).
- [37] *Time-Dependent Density Functional Theory*, Lecture Notes in Physics, edited by M. A. L. Marques, C. A. Ullrich, F. Nogueira, A. Rubio, K. Burke, and E. K. U. Gross (Springer-Verlag, Berlin, 2006), Vol. 706.
- [38] *Fundamentals of Time-Dependent Density Functional Theory*, Lecture Notes in Physics, edited by M. A. L. Marques, N. T. Maitra, F. M. S. Nogueira, E. K. U. Gross, and A. Rubio, (Springer, Heidelberg, 2012), Vol. 837.
- [39] R. Balian and M. Vénéroni, Lyapunov stability and Poison structure of the thermal TDHF and RPA, *Ann. Phys. (NY)* **195**, 324 (1989).
- [40] A. Bulgac, M. M. Forbes, and W. Wlazłowski, Towards quantum turbulence in cold atomic fermionic superfluids, *J. Phys. B: At., Mol. Opt. Phys.* **50**, 014001 (2016).
- [41] A. Bulgac, Time-dependent density functional theory for fermionic superfluids: from cold atomic gases, to nuclei and neutron star crust, *Phys. Status Solidi B* **256**, 1800592 (2019).
- [42] S. Jin, K. J. Roche, I. Stetcu, I. Abdurrahman, and A. Bulgac, The LISE package: Solvers for static and time-dependent superfluid local density approximation equations in three dimensions, *Comput. Phys. Commun.* **269**, 108130 (2021).
- [43] P. Ring and P. Schuck, *The Nuclear Many-Body Problem*, 1st ed., Theoretical and Mathematical Physics Series No. 17 (Springer-Verlag, Berlin, Heidelberg, New York, 2004).
- [44] G. F. Bertsch, “The Many-Body Challenge Problem (MBX) formulated in 1999,” see also Ref. [45].
- [45] G. A. Baker, Jr., Neutron matter model, *Phys. Rev. C* **60**, 054311 (1999).
- [46] *The BCS–BEC Crossover and the Unitary Fermi Gas*, Lecture Notes in Physics, edited by W. Zwerger (Springer-Verlag, Berlin Heidelberg, 2012), Vol. 836.
- [47] J. Carlson, S. Gandolfi, K. E. Schmidt, and S. Zhang, Auxiliary field quantum Monte Carlo for strongly paired fermions, *Phys. Rev. A* **84**, 061602(R) (2011).
- [48] M. J. H. Ku, A. T. Sommer, L. W. Cheuk, and M. W. Zwierlein, Revealing the superfluid lambda transition in the universal thermodynamics of a unitary fermi gas, *Science* **335**, 563 (2012).
- [49] A. Bulgac, Local-density-functional theory for superfluid fermionic systems: The unitary gas, *Phys. Rev. A* **76**, 040502(R) (2007).
- [50] A. Bulgac, M. M. Forbes, and P. Magierski, “The unitary Fermi gas: From Monte Carlo to density functionals,” Chap. 9, pp. 127–191, Vol. 836 of Ref. [46] (2012).
- [51] E. A. Yuzbashyan and M. Dzero, Dynamical Vanishing of the Order Parameter in a Fermionic Condensate, *Phys. Rev. Lett.* **96**, 230404 (2006).
- [52] E. A. Yuzbashyan, O. Tsypliyatyev, and B. L. Altshuler, Relaxation and Persistent Oscillations of the Order Parameter in Fermionic Condensates, *Phys. Rev. Lett.* **96**, 097005 (2006).
- [53] E. A. Yuzbashyan, Normal and anomalous solitons in the theory of dynamical Cooper pairing, *Phys. Rev. B* **78**, 184507 (2008).
- [54] A. Bulgac and S. Yoon, Large Amplitude Dynamics of the Pairing Correlations in a Unitary Fermi Gas, *Phys. Rev. Lett.* **102**, 085302 (2009).
- [55] A. Bulgac, Y.-L. Luo, P. Magierski, K. J. Roche, and Y. Yu, Real-time dynamics of quantized vortices in a unitary Fermi superfluid, *Science* **332**, 1288 (2011).
- [56] A. Bulgac, Michael McNeil Forbes, M. M. Kelley, K. J. Roche, and G. Wlazłowski, Quantized Superfluid Vortex Rings in the Unitary Fermi Gas, *Phys. Rev. Lett.* **112**, 025301 (2014).
- [57] G. Wlazłowski, A. Bulgac, Michael McNeil Forbes, and K. J. Roche, Life cycle of superfluid vortices and quantum turbulence in the unitary Fermi gas, *Phys. Rev. A* **91**, 031602(R) (2015).
- [58] G. Wlazłowski, K. Sekizawa, M. Marchwiany, and P. Magierski, Suppressed Solitonic Cascade in Spin-Imbalanced Superfluid Fermi Gas, *Phys. Rev. Lett.* **120**, 253002 (2018).
- [59] T. Yefsah, A. T. Sommer, M. J. H. Ku, L. W. Cheuk, W. Ji, W. S. Bakr, and M. W. Zwierlein, Heavy solitons in a fermionic superfluid, *Nature (London)* **499**, 426 (2013).
- [60] M. J. H. Ku, W. Ji, B. Mukherjee, E. Guardado-Sanchez, L. W. Cheuk, T. Yefsah, and M. W. Zwierlein, Motion of a Solitonic Vortex in the BEC-BCS Crossover, *Phys. Rev. Lett.* **113**, 065301 (2014).
- [61] I. Stetcu, A. Bulgac, P. Magierski, and K. J. Roche, Isovector giant dipole resonance from the 3D time-dependent density functional theory for superfluid nuclei, *Phys. Rev. C* **84**, 051309(R) (2011).
- [62] I. Stetcu, C. A. Bertulani, A. Bulgac, P. Magierski, and K. J. Roche, Relativistic Coulomb excitation within Time Dependent Superfluid Local Density Approximation, *Phys. Rev. Lett.* **114**, 012701 (2015).
- [63] A. Bulgac, P. Magierski, K. J. Roche, and I. Stetcu, Induced Fission of  $^{240}\text{Pu}$  within a Real-Time Microscopic Framework, *Phys. Rev. Lett.* **116**, 122504 (2016).

- [64] G. Wlazłowski, K. Sekizawa, P. Magierski, A. Bulgac, and Michael McNeil Forbes, Vortex Pinning and Dynamics in the Neutron Star Crust, *Phys. Rev. Lett.* **117**, 232701 (2016).
- [65] A. Bulgac and S. Jin, Dynamics of Fragmented Condensates and Macroscopic Entanglement, *Phys. Rev. Lett.* **119**, 052501 (2017).
- [66] A. Bulgac, S. Jin, K. J. Roche, N. Schunck, and I. Stetcu, Fission dynamics of  $^{240}\text{Pu}$  from saddle to scission and beyond, *Phys. Rev. C* **100**, 034615 (2019).
- [67] A. Bulgac, S. Jin, and I. Stetcu, Nuclear fission dynamics: Past, present, needs, and future, *Front. Phys.* **8**, 63 (2020).
- [68] R. P. Feynman, Application of quantum mechanics to liquid helium, *Prog. Opt.* **1**, 17 (1955).
- [69] *Quantized Vortex Dynamics and Superfluid Turbulence*, edited by C. F. Barenghi, R. J. Donnelly, and W. F. Vinen (Springer, Berlin, 2001).
- [70] G. Wlazłowski, Link for the W-SLDA package, <http://wsllda.fizyka.pw.edu.pl> (2020).
- [71] P. Magierski, G. Wlazłowski, A. Bulgac, and J. E. Drut, Finite-Temperature Pairing Gap of a Unitary Fermi Gas by Quantum Monte Carlo Calculations, *Phys. Rev. Lett.* **103**, 210403 (2009).
- [72] P. Magierski, G. Wlazłowski, and A. Bulgac, Onset of a Pseudogap Regime in Ultracold Fermi Gases, *Phys. Rev. Lett.* **107**, 145304 (2011).
- [73] G. Wlazłowski, P. Magierski, A. Bulgac, and K. J. Roche, Temperature evolution of the shear viscosity in a unitary Fermi gas, *Phys. Rev. A* **88**, 013639 (2013).
- [74] G. Wlazłowski, P. Magierski, J. E. Drut, A. Bulgac, and K. J. Roche, Cooper Pairing Above the Critical Temperature in a Unitary Fermi Gas, *Phys. Rev. Lett.* **110**, 090401 (2013).
- [75] A. Richie-Halford, J. E. Drut, and A. Bulgac, Emergence of a Pseudogap in the BCS-BEC Crossover, *Phys. Rev. Lett.* **125**, 060403 (2020).
- [76] G. Wlazłowski, W. Quan, and A. Bulgac, Perfect-fluid behavior of a dilute Fermi gas near unitary, *Phys. Rev. A* **92**, 063628 (2015).
- [77] A. Bulgac, J. E. Drut, and P. Magierski, Spin 1/2 Fermions in the Unitary Regime: A Superfluid of a New Type, *Phys. Rev. Lett.* **96**, 090404 (2006).
- [78] A. Bulgac, J. E. Drut, and P. Magierski, Quantum Monte Carlo simulations of the BCS-BEC crossover at finite temperature, *Phys. Rev. A* **78**, 023625 (2008).
- [79] J. E. Drut, T. A. Lähde, G. Wlazłowski, and P. Magierski, Equation of state of the unitary Fermi gas: An update on lattice calculations, *Phys. Rev. A* **85**, 051601(R) (2012).
- [80] O. Hahn and F. Strassmann, Über den Nachweis und das Verhalten der bei der Bestrahlung des Urans mittels Neutronen entstehenden Erdalkalimetalle, *Naturwissenschaften* **27**, 11 (1939).
- [81] N. Bohr, Neutron capture and nuclear constitution, *Nature* **137**, 344 (1936); News and Views (editorial), *ibid.* **137**, 351 (1936).
- [82] L. Meitner and O. R. Frisch, Disintegration of uranium by neutrons: A new type of nuclear reaction, *Nature (London)* **143**, 239 (1939).
- [83] E. Fermi, On the origin of the cosmic radiation, *Phys. Rev.* **75**, 1169 (1949).
- [84] R. Balian and M. Vénéroni, Fluctuations in a time-dependent mean-field approach, *Phys. Lett. B* **136**, 301 (1984).
- [85] R. Balian, P. Bonche, H. Flocard, and M. Vénéroni, Mass dispersions in a time-dependent mean-field approach, *Nucl. Phys. A* **428**, 79 (1984).
- [86] R. Balian and M. Vénéroni, Time-dependent variational principle for the expectation value of an observable: Mean-field applications, *Ann. Phys. (NY)* **164**, 334 (1985).
- [87] C. Simenel, Particle-Number Fluctuations and Correlations in Transfer Reactions Obtained Using the Balian-Vénéroni Variational Principle, *Phys. Rev. Lett.* **106**, 112502 (2011).
- [88] C. Simenel, Nuclear quantum many-body dynamics, *Eur. Phys. J. A* **48**, 152 (2012).
- [89] G. Scamps, C. Simenel, and D. Lacroix, Superfluid dynamics of  $^{258}\text{Fm}$  fission, *Phys. Rev. C* **92**, 011602(R) (2015).
- [90] E. Williams, K. Sekizawa, D. J. Hinde, C. Simenel, M. Dasgupta, I. P. Carter, K. J. Cook, D. Y. Jeung, S. D. McNeil, C. S. Palshetkar, D. C. Rafferty, K. Ramachandran, and A. Wakhle, Exploring Zeptosecond Quantum Equilibration Dynamics: from Deep-Inelastic to Fusion-Fission Outcomes in  $^{58}\text{Ni} + ^{60}\text{Ni}$  Reactions, *Phys. Rev. Lett.* **120**, 022501 (2018).
- [91] A. Volya and V. Zelevinsky, Time-dependent relaxation of observables in complex quantum systems, *J. Phys. Complex.* **1**, 025007 (2020).